Pathogenic Sequence for Dissecting Aneurysm Formation in a Hypomorphic Polycystic Kidney Disease 1 Mouse Model

Sabrine Hassane, Nanna Claij, Irma S. Lantinga-van Leeuwen, J. Conny Van Munsteren, Natascha Van Lent, Roeland Hanemaaijer, Martijn H. Breuning, Dorien J.M. Peters, Marco C. DeRuiter

Objective—Autosomal Dominant Polycystic Kidney Disease (ADPKD) is a multi-system disorder characterized by progressive cyst formation in the kidneys. Serious complications of ADPKD are intracranial and aortic aneurysms. The condition is mainly caused by mutations in the *PKD1* or *PKD2* gene. We have carefully analyzed vascular remodeling in hypomorphic $Pkd1^{nl/nL}$ mouse model with dissecting aneurysms in the aorta.

Methods and Results—Quantitative real-time polymerase chain reaction revealed that in the aorta the expression of normal *Pkd1* is reduced to approximately 26%. Using (immuno)histochemistry we have characterized the pathogenetic sequence for dissecting aneurysm formation. The aorta shows regions with accumulation of matrix components between the elastin lamellae. This is followed by increased numbers of smooth muscle cells and locally weakening of the media. In the intima, accumulation of matrix components and detachment of endothelial cells from the elastin lamellae results in a tear. The combination of weak media and a tear in the intima leads to rupture of the vessel wall resulting in intramural bleeding.

Conclusions—The $Pkd1^{nl/nl}$ mouse reveals that polycystin1 is implicated in maintenance of the vessel wall structural integrity, and it is a useful model for dissecting aneurysm formation studies. (***Arterioscler Thromb Vasc Biol.* 2007;27:2177-2183.**)

Key Words: dissecting aneurysm ■ polycystic kidney disease ■ aorta ■ extracellular matrix ■ *Pkd1*

Autosomal Dominant Polycystic Disease (ADPKD) is one of the most common genetic diseases. ADPKD affects 1 in 1000 individuals and is characterized by progressive development of renal cysts and an increased risk of aneurysm formation. The prevalence of cerebral aneurysms in ADPKD patients is approximately 10-fold higher than in the general population and about 27% among ADPKD patients with a family history for aneurysms.[1,2] The few clinical studies done to determine the frequency of aortic aneurysms in ADPKD, suggest a prevalence varying from 1% to 10% in ADPKD patients.[3–5] Furthermore, a gene expression profile study revealed a decrease of *PKD1* expression in dissected human aortas.[6] ADPKD has been associated with mutations in the *PKD1* or *PKD2* gene, encoding the proteins polycystin1 and polycystin2. Both genes are expressed in the smooth muscle cells (SMCs) and endothelial cells (ECs) of the blood vessel.[7–9] At present, however, hardly any histopathologic analyses on dissections and aneurysms in ADPKD have been performed.

Several *Pkd1* and *Pkd2* knock-out mouse models have been generated, however knock-out embryos die at embryonic days 13.5 to 14.5 from a primary cardiovascular defect.[9–12] These embryos show edema, focal vascular leaks, and hemorrhage. The fact that these mice die *in utero* withholds the possibility to study aneurysm formation in ADPKD. Recently, we have generated a *Pkd1* hypomorphic mouse model, $Pkd1^{nl/nl}$, with reduced *Pkd1* transcripts in the kidneys.[13] $Pkd1^{nl/nl}$ mice are viable, and the majority of the animals die within 1 to 2 months after birth. These mice show dissecting aneurysms and cysts in kidneys, liver, and pancreas, which is in line with the pathogenic features found in the human ADPKD phenotype. $Pkd1^{nl/nl}$ mice are the first viable ADPKD mice with spontaneous dissecting aneurysm formation in the aorta enabling studies on vascular remodeling in ADPKD. In this study we have carefully characterized dissecting aneurysm formation in these hypomorphic mice. Reduced levels of *Pkd1* transcripts measured in the aorta indicate a direct association between *Pkd1* and vessel wall integrity.

Materials and Methods

Animals and Tissue Preparation

The generation of $Pkd1^{nl/nl}$ mice has been described in detail by Lantinga-van Leeuwen et al.[13] A *loxP*-flanked neomycin selection-

Original received May 30, 2006; final version accepted June 25, 2007.

From the Center for Human and Clinical Genetics (S.H., N.C., I.S.L.L., M.H.B., D.J.M.P.), the Department of Anatomy and Embryology (J.C.V.M., M.C.D.), Leiden University Medical Center, and the Gaubius Laboratory (N.V.L., R.H.), TNO BioSciences, Leiden, The Netherlands.

D.J.M.P. and M.C.D. contributed equally to this study.

Correspondence to Dr D.J.M. Peters, Department of Human Genetics, Center for Human and Clinical Genetics, Leiden University Medical Center, Postal zone: S-04-P, P.O. Box 9600, 2300 RC, Leiden, The Netherlands. E-mail d.j.m.peters@lumc.nl

Arterioscler Thromb Vasc Biol. **is available at http://atvb.ahajournals.org** **DOI: 10.1161/ATVBAHA.107.149252**

cassette was inserted into intron 1 of the *Pkd1* gene by homologous recombination, and a third *loxP* site was inserted in intron 11. Chimeric offspring were backcrossed with C57Bl/6Jico mice 3 to 6 times. Histological analysis was performed on 9 $Pkd1^{nl/nl}$ (5 male and 4 female) and 5 (3 male and 2 female) control mice at the age of 1 month and 3 $Pkd1^{nl/nl}$ (1 male and 2 female) at the age of 1 week. The aortas, from aortic root to the bifurcation of the iliac arteries, were carefully dissected and fixed in 98% ethanol absolute with 2% acetic acid or in 4% paraformaldehyde in 0.1 mol/L phosphate buffer (pH7.4). In 1 $Pkd1^{nl/nl}$ mouse only the abdominal aorta was not dissected. Fixed tissues were dehydrated in graded ethanol and xylene and embedded in paraffin. Five-micrometer sections of the complete ascending and descending aorta were completely mounted serially onto glass slides.

Antibodies

SM-α-actin (1A4) 1:2000 (Sigma), Collagen I and III 1:200 (Sanbio), Fibrillin-1 1: 500 (a generous gift from R. Mecham, Washington), Fibronectin 1:4000 (a generous gift from B.N. Bachera, Leiden, The Netherlands), Isolectin 1:20 (Sigma-Aldrich Chemie), Osteopontin 1:100 (a generous gift from L.W. Fisher, Bethesda, Md), Perlecan, Versican alpha and beta 1:20 (a generous gift from J.R. Hassell, Pittsburgh, Pa), Rabbit-anti-mouse Macrophage (AIA 31240) 1:200 (Accurate Chemical and scientific), matrix metalloproteinase (MMP)-2 Ab-4 (75 to 7F7) 1:4 (Calbiochem), MMP-9 11A-5 (11A-5) 1: 100 (Neo Markers), Ki-67 1:3000 (Novocastra), terminal deoxynucleotidyl transferase-mediated dUTP nick end-labeling (TUNEL) 1:14 (Roche). Secondary antibodies: Rabbit-anti-mouse HRP 1:200, Swine-anti-rabbit HRP 1:200 (DAKO), Goat-anti-rabbit 1:50, Rabbit-peroxidase-anti-peroxidase 1:250 (Nordic Immunologic Laboratories), mouse-biotinylated (ABC-kit vectastain; Brunschwig Chemie).

Immunohistochemistry

After deparaffinization, sections were stained using standard procedures.[14] The antibody complexes were visualized using 0.04% diaminobenzidine-tetra-hydrochloride (DAB; Sigma). Antigen retrieval was applied for fibronectin and ki67 staining and for monoclonal antibody 1A4 (SM-α-actin) a complex with the secondary antibody was prepared before incubation. The following histological stainings were performed: Hematoxylin Eosin (HE), Resorcin Fuchsin (RF) for elastin lamellae, Alcian blue for staining glycosaminoglycans and thereby the proteoglycans, von Kossa and alizarin red for calcium deposition and Sirius red for collagen. For details please see the supplemental materials, available online at http://atvb.ahajournals.org.

RNA Analysis

Complete aortas and kidneys of 5 control and 6 hypomorphic mice at the age of 1 month were dissected. Total RNA was isolated and used in a quantitative real-time reverse transcriptase PCR. For detailed protocol please see the supplemental materials.

Aortic Volume Measurements

To measure the volumes of aortic walls (including the dissection) and aortic lumens, we used the volume counting method according to Cavalieri. For details please see the supplemental materials.

Zymography

Whole aortas of 4 mutant and 3 wild-type mice were powdered in liquid nitrogen, and a tissue extract was made in 50 mmol/L Tris pH 7.7, 1.5 mmol/L NaCl and 0.25% Triton X100. MMPs expression was analyzed by zymography. For details please see the supplemental materials.

Results

Analysis of Aortic *Pkd1* mRNA Levels

We used $Pkd1^{nl/nl}$ mice containing a *loxP*-flanked neomycin selection-cassette in intron 1 of the *Pkd1* gene. We previously have shown that a fragment of the neomycin cassette is incorporated in a fraction of the *Pkd1* transcripts by alternative splicing in the kidneys, resulting in a frame shift and predicted to result in an early premature translation stop.[13] This results in a reduction of the normal *Pkd1* expression. Here we determined the level of normal *Pkd1* in the aortas of hypomorphic and wild-type mice with a real-time PCR assay. In mutant mice, the expression of normal *Pkd1* is reduced to approximately 26% in the aortas and 37% in the kidneys of the same mice (Figure 1A). The total *Pkd1* expression (normal plus mutant *Pkd1*) in the $Pkd1^{nl/nl}$ mice is about 1.5 and 2.7 times-fold increased in aorta and kidney, respectively (Figure 1B). In aortas of $Pkd1^{nl/nl}$ mice the ratio of normal versus total *Pkd1* expression is approximately 0.13, indicating that only 13% of the total *Pkd1* transcript is normal. The same ratio was found in the kidneys.

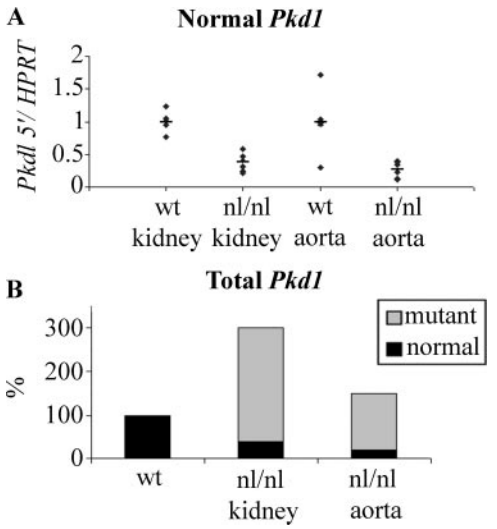

Figure 1. Quantitative real-time PCR analysis of renal and aortic RNA samples of 5 wild-type and 6 $Pkd1^{nl/nlL}$ mice. A, Expression of normal *Pkd1* transcript. The 5′ *Pkd1* PCR amplifies normal *Pkd1* transcripts. 5′ *Pkd1* vs *HPRT* is normalized to the mean ratio of 5 wild-type mice, which has been set to 1. The expression of normal *Pkd1* transcript in the aorta and kidney of $Pkd1^{nl/nl}$ mice is reduced to 26% and 37%, respectively. B, Total *Pkd1* transcript. The 3′ *Pkd1* PCR amplifies both mutant and normal *Pkd1* transcripts. 3′ *Pkd1* vs *HPRT* is normalized to the mean ratio of 5 wild-type mice, which has been set to 1. The total *Pkd1* transcript is about 1.5 and 2.7 times increased in aorta and kidney of $Pkd1^{nl/nl}$ mice, respectively. In both kidney and aorta, about 13% of the total transcript is normal.

Characterization of Aortic Pathology in $Pkd1^{nl/nl}$ Mice

Eight of the 9 examined $Pkd1^{nl/nl}$ mice showed 1 or more abnormalities with different severity at different regions in the descending thoracic and abdominal aorta. Dissections with intramural bleeding were detected in 5 mice. Five mice had progressive dissecting aneurysms showing pseudo lumens all over the descending aorta (3 mice; Figure 2A) or caudal mesenteric artery (2 mice). Two mice showed a local intramural bleeding (Figure 2B). The dissections in the caudal mesenteric arteries were ruptured leading to retroperitoneal bleeding. The volume of the vessel wall in the areas of these progressive dissections was significantly increased in both the thoracic and abdominal aorta compared with the wild-type aortas of the same regions. However, the inner vessel lumen was not changed (Figure 3A and 3B).

The ascending aorta and segment B, which is located between the left carotid and the left subclavia in the aortic

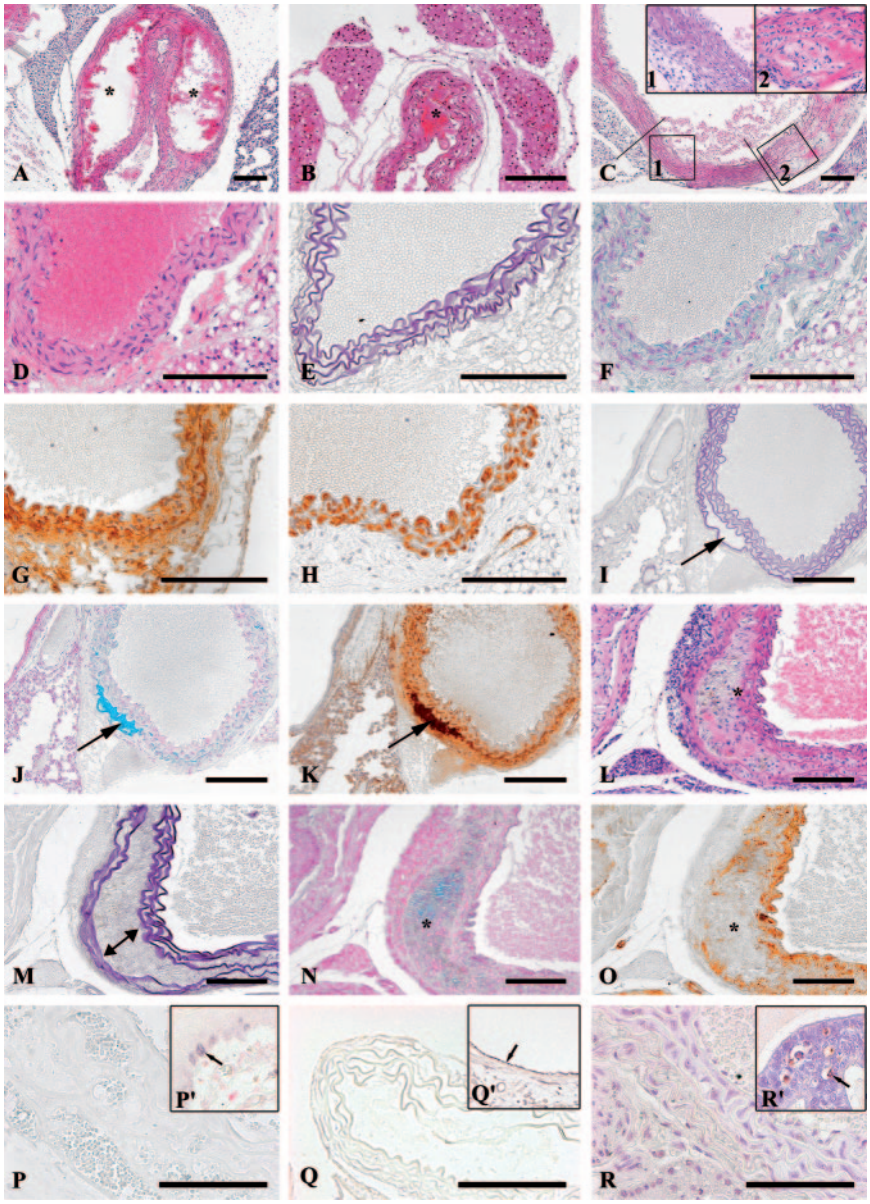

Figure 2. Dissecting aneurysms in *Pkd1*$^{nl/nl}$ mice. A–C, Hematoxylin Eosin. A, Progressive dissection with 2 pseudo lumens (asterisk) filled with blood. B, Local dissection with intramural bleeding (asterisk). Segment B did not show abnormalities whereas (C1) the surrounding region showed progressive media thickening (C2). D–H, Wild-type aorta: D, Hematoxylin Eosin; E, Resorcin Fuchsin; F, Alcian blue; G, fibronectin; H, SM-α-actin. I–K, Sequential sections showing mild medial thickening: I, Resorcin Fuchsin; J, Alcian blue; K, fibronectin. The elastin lamellae are disjoined (arrow; I) showing accumulation of proteoglycans (J) and fibronectin (K) between the elastin lamellae (arrows). L–O, Progressive stages of medial degenerative changes in *Pkd1*$^{nl/nl}$ mice: L, Hematoxylin Eosin; M, Resorcin Fuchsin; N, Alcian blue; O, SM-α-actin. At more progressive regions, media thickening with increased SMCs between the elastin lamellae is found (L), however the elastin lamellae are still intact (M). At these regions proteoglycans are increased (N) whereas SM-α-actin is decreased (O; asterisks). Ki67 showed no proliferation (P), whereas the basal cells of the esophagus did stain positive (arrow; P′). MMP-2 (Q) and TUNEL (R) were both negative in these regions, whereas the positive control was positive, cystic kidney (Q′) and prostate tissue (arrows; R′), respectively. Bar=100 μm.

arch, were normal. One mouse showed media thickening in the whole area of the aortic arch and descending thoracic aorta except for segment B and the ascending aorta (Figure 2C). In these 2 normal regions SMCs seemed to keep their connection with the matrix, whereas the surrounding region of the aorta showed media thickening with disjoined elastin lamellae. One mouse showed local progressive medial thickening in the abdominal aorta without intramural bleeding.

In addition to dissecting aneurysms, all descending aortas studied contained normal vessel wall structure and incomplete dissections. Medial thickening was found in the thoracic aorta of 6 mice, in the abdominal aorta of 2 mice and intima thickening was found in the thoracic aorta of 1 mouse and in the abdominal aorta of 2 mice. The abnormalities found, were of varying pathological severity. This allowed us to describe the sequential order of events occurring in the media and intima, resulting in a dissecting aneurysm.

Media Thickening in *Pkd1*$^{nl/nl}$ Aortas

The media of the aorta of wild-type mice consists of 5 to 6 layers of SMCs alternated with concentric sheets of elastin lamellae (Figure 2D, 2E, and 2H). Surrounding the SMCs extracellular matrix molecules like proteoglycans and fibronectin are present (Figure 2F and 2G). Examination of elastin lamellae in *Pkd1*$^{nl/nl}$ aortas by Resorcin Fuchsin staining showed an increase in the space between the lamellae without any fragmentation of the lamellae (Figure 2I). The expression levels of proteoglycans and fibronectin were both notably increased in these regions (Figure 2J and 2K) compared with wild-type aortas (Figure 2F and 2G). The proteoglycans versican and perlecan have been shown to be increased in cultures of medial smooth muscle cells from tissue affected by abdominal aortic aneurysm.[15] In our mouse model perlecan was increased whereas versican was absent in both wild-type and mutant mice. Using immunohistochemis-

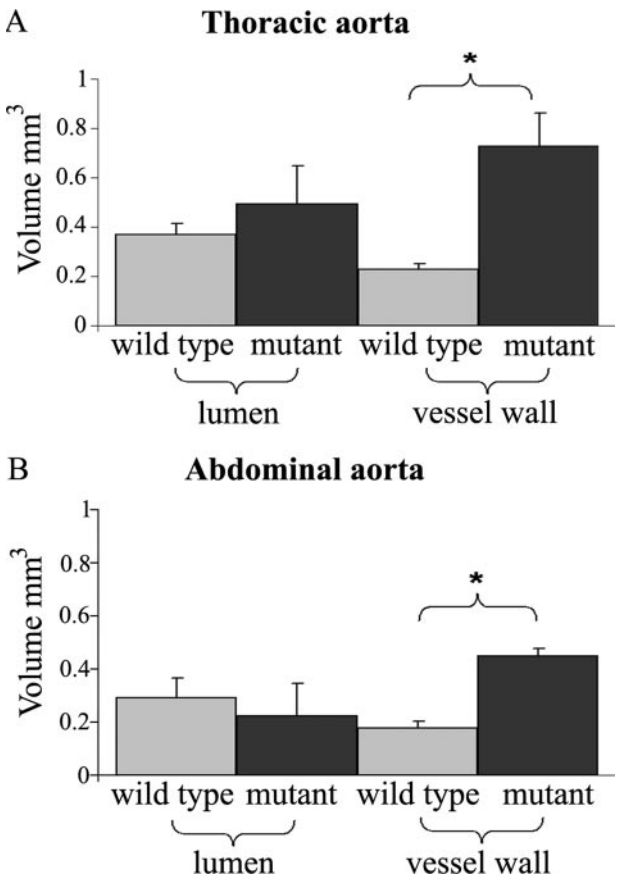

Figure 3. Volume measurements of aortic lumen and vessel wall in thoracic (A) and abdominal aortas (B). The volume of vessel wall in both the thoracic and abdominal aortas is increased. The volume of the inner vascular lumens of wild-type mice is not significantly different from mutant mice. *$P<0.05$.

try no MMP-2 and 9 expression was detected in the wild-type or *Pkd1*$^{nl/nl}$ aortas (Figure 2Q). Zymography, which is a more sensitive method than immunohistochemistry, revealed none to a very low and similar MMP-2 and MMP-9 expression in both, mutant and wild-type, aortas (supplemental Figure I). At other more progressive regions in the aortas, the elastin lamellae were more disjoined with an increased number of smooth muscle cells in between (Figure 2L). However, the elastin lamellae were still intact (Figure 2M). The SMCs were disarranged with a low SM–α-actin expression (Figure 2O). Few SMCs had condensed nuclei, however these cells did not stain positive for TUNEL (Figure 2R). Macrophage staining did not reveal any immune-infiltrate in this region (Table). No accumulation of fibronectin was detected in this region. However, proteoglycans were still increased (Figure 2N). The distribution of collagen and fibrillin 1 in the vessel wall of *Pkd1*$^{nl/nl}$ mice was comparable to wild-type mice. No calcification or expression of osteopontin was detected in all vessels analyzed (Table).

Intima Thickening in *Pkd1*$^{nl/nl}$ Aortas

The wild-type intima consists of a single layer of flattened endothelial cells on a basal membrane and a subjacent elastin lamellae known as internal elastic lamina. Histological analysis of the intima of *Pkd1*$^{nl/nl}$ by Hematoxylin Eosin showed detachment of the ECs from the internal elastic lamina (Figure 4A and 4B). At these regions isolectin staining was decreased indicating a decreased number of ECs or decreased expression of this marker on ECs (Figure 4C and 4D). In other regions the subendothelial region was filled with proteoglycans and the cell numbers were increased (Figure 4E). However, the accumulation of proteoglycans is neither attributable to an increase in versican or perlecan nor did it coincide with increased fibronectin expression as observed in the media thickening (Table). One of the mice showed a tear in the intima next to the degenerative changes within the media resulting into a progressive dissection all over the aorta (Figure 4F). At the entrance of dissection, fragmentation of the elastin lamellae was found, allowing the blood to spread through the aortic media. Despite substantial effort, we could not locate the exact site of rupture in the other animals.

Dissecting Aneurysm

Abnormalities in the media and intima were identified in different regions of the aorta, indicating that the reduction of *Pkd1* in both SMCs and ECs contributes to the formation of dissecting aneurysms by 2 processes, 1 in the media and the other in the intima. It is not clear whether the initial event of a dissecting aneurysm occurs in the intima or media. We hypothesize that on reducing the expression of polycystin1, the stability of the contact between SMCs and extracellular matrix molecules is reduced. This may disturb some cellular events in the SMCs resulting in a phenotypic change toward a more synthetic phenotype, which means that they produce more matrix components, which accumulate between the elastin lamellae, and start to hyperproliferate (Figure 5B). This results in an increased thickening of the media, which will become weaker (Figure 5C). In the intima the endothelial cells detach from the elastin lamellae (Figure 5D). The number of intima cells increases and the matrix components accumulate in the subendothelial region (Figure 5E). The final event allowing the blood to spread through the aortic media is the tear of the intima (Figure 5F and 5G). When present, next to the degenerative changes within the media, the resistance of the aortic wall to hemodynamic stress reduces, leading to dissection (Figure 5H).

Discussion

The *Pkd1*$^{nl/nl}$ mice provided a new model to study aortic dissecting aneurysm formation in ADPKD. It also confirmed the role of *Pkd1* in dissecting aneurysm formation. Our mouse model represents a very severe phenotype of ADPKD with dissections in the aorta, probably due to the fact that the overall *Pkd1* expression in the *Pkd1*$^{nl/nl}$ mice is lower than in human ADPKD patients. In patients 1 wild-type *Pkd1* allele is present, whereas in the aortas of these *Pkd1*$^{nl/nl}$ mice normal *Pkd1* transcripts is approximately 75% reduced (Figure 1A). All dissections were found in the descending aorta whereas the ascending aorta was normal. This is in line with the humane phenotype, as most dissections are found in the descending aorta of ADPKD patients.[3–5] Although intracranial saccular aneurysms are more common in ADPKD than aortic aneurysms, no intracranial aneurysms were found in 3 *Pkd1*$^{nl/nl}$ mice at the age of 1 month (data not shown).

Table. Immunohistochemical Characterization of *Pkd1*$^{nl/nl}$ Mice Compared to Wild-Type

	Normal Media	Media Thickening	Normal Intima	Intima Thickening
SM-alpha-actin	+	+/−	−	−
Isolectin	−	−	+	+/−
Collagen I	+	+	+	+
Collagen III	+	+	+	+
Collagen	+	+	+	+
Fibrillin I	+	+	+	+
Elastin	+	+*	+	+*
Fibronectin	+	++	+	+
Osteopontin	−	−	−	−
Calcium deposition	−	−	−	−
Perlecan	+	++	−	−
Versican	−	−	−	−
Proteoglycans	+	++	−	+/−
Macrophages	−	−	−	−
MMP-2	−	−	−	−
MMP-9	−	−	−	−
Ki-67	−	−	−	−
TUNEL	−	−	−	−

*Elastin lamellae were diverged/broken. − indicates no expression.

Probably, intracranial aneurysms need more time to develop or the method used (immunohistochemistry) is not sensitive enough to detect small saccular aneurysms, or additional factors as elevated blood pressure are essential to develop these kind of aneurysms. Interestingly, in 6- to 9-month-old *Pkd2*$^{\pm}$ mice, Q. Qian et al observed macroscopic intracranial vascular complications after induction of hypertension.[16]

A direct correlation between MMP-mediated elastin degradation and elastin calcification has been reported. Perivascular administration of $CaCl_2$ to abdominal aortas induced calcification and degradation of elastin fibers.[17] Focal linear calcifications were also detected in a mouse model with reduction of fibrillin-1 showing fragmentation of elastin lamellae and MMP-9 expression.[18] Our data fit into this correlation. In our mouse model MMP-2 and MMP-9 expression was very low, comparable with wild-type expression, and no elastin calcification or elastin degradation were found in the media thickening. In addition, we did not observe influx of inflammatory cells which are the main source of MMPs secretion. These properties of dissecting aneurysm formation in *Pkd1*$^{nl/nl}$ mice, therefore, seem to be distinct from other models.

Polycystin1 has been found to be a component of large multiprotein complexes associated with cell-matrix contact at focal adhesions in cultures of renal epithelial cells. It is also associated with adherence junctions and desmosomes in confluent cultures of the renal epithelial cell line Madin-Darby canine kidney (MDCK).[19–21] Polycystin1 is also implicated in SMC-elastin contact. The expression of *Pkd1* is found in dense plaques, which are analogous to focal adhesions in epithelial cells and attach the intracellular contractile filaments of SMCs to the elastin lamellae.[22,23] In our *Pkd1*$^{nl/nl}$ mice a widened space between the elastin lamellae was found, suggesting loss of contact between SMCs and elastin or other extra cellular matrix structures. Loss of physical contacts, and hence signals from these interactions, is associated with a phenotypic change toward a more synthetic phenotype of the SMCs.[24] Furthermore, loss of the SMC-elastin interaction may increase SMC proliferation as elastin has a regulatory function controlling SMC proliferation.[25] All these features are found in our *Pkd1*$^{nl/nl}$ mouse model, confirming this regulatory mechanism. Although we did not detect ki67-positive cells in the sections available for analysis, eg, very early stages and dissections (Figure 2P), cell proliferation should have occurred because increased cell layers were present at certain stages of dissection formation (Figure 2L) and these cells did not stain for inflammatory cells. The decreased expression of SM-α-actin and increased expression of proteoglycans and fibronectin in the *Pkd1*$^{nl/nl}$ mouse model indicate a response toward a more synthetic phenotype. Polycystin1 might be involved in a SMC-matrix adhesion molecule complex, which maintains a stable SMC phenotype and thereby maintaining the structural vessel wall integrity.

Notably, no media thickening was found in segment B of the aortic arch of our mutant mice. The areas adjacent to segment B showed a progressive media thickening, suggesting a normal SMC-matrix contact in this segment (Figure 2C). In wild-type mice the media of this segment shows characteristics in which it differs from the rest of the aorta. It is negative for SM-α-actin and has extensive medial innervations. These SMCs have also a different embryonic origin compared with the descending aorta as it is derived from the fourth pharyngeal artery in the embryonic thoracic arterial tree.[14,26] Interestingly, lowering the *Pkd1* expression did not show any influence on the structure of this vessel segment. *Pkd1* expression may not be critical in maintaining the structural vessel wall integrity in the aortic B-segment.

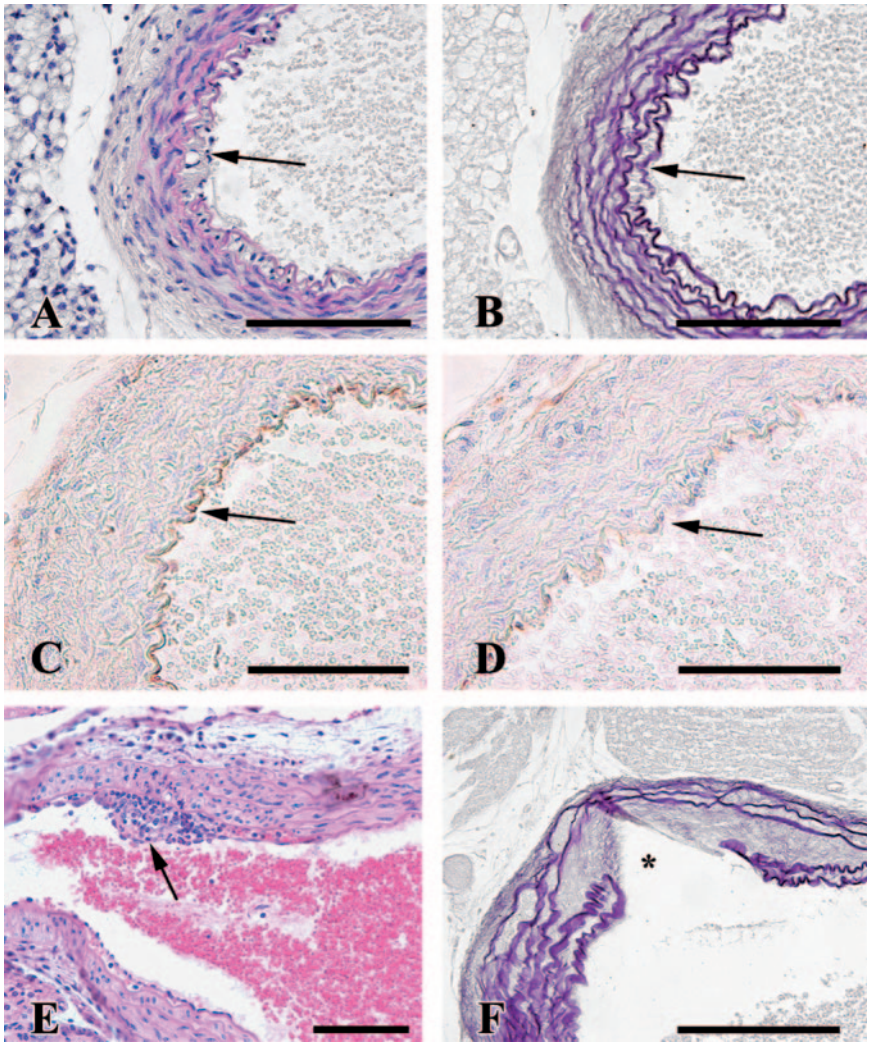

Figure 4. Histopathologic appearance of the intima in *Pkd1*$^{nl/nl}$ mice. A–G, Sequential sections showing different stages of intima degenerative changes in *Pkd1*$^{nl/nl}$ mice. ECs detach from the internal elastic lamellae (A) and the internal elastic lamina is less compact (B; arrows). At these regions isolectin is decreased (D) compared with control (C; arrows). At more severe regions subendothelial thickening is found (E; arrow). At the entrance of the dissection, the elastin lamellae are broken (F; asterisks). A, E Hematoxylin Eosin; C, D isolectin; B, F Resorcin Fuchsin. Bar=100 μm.

Both polycystin1 and 2 are probably involved in mechanosensing as they are localized in the primary cilia in renal cells.[27] Polycystin1 is also concentrated around centrioles and in particles along primary cilia of human umbilical vein endothelial cells (HUVECs).[28] Recently, monocilia were demonstrated on a subset of endothelial cells in low-shear regions.[29] In addition, polycystin1 has been shown to colocalize with platelet-endothelial cell adhesion molecule-1 (PECAM-1), a cell adhesion molecule also found to be involved in mechanosensing mechanism on the cell membrane.[30,31] PECAM-1 also maintains adherens junction integrity and permeability. The latter function may be influenced by *Pkd1* expression, as *Pkd1* knock-out

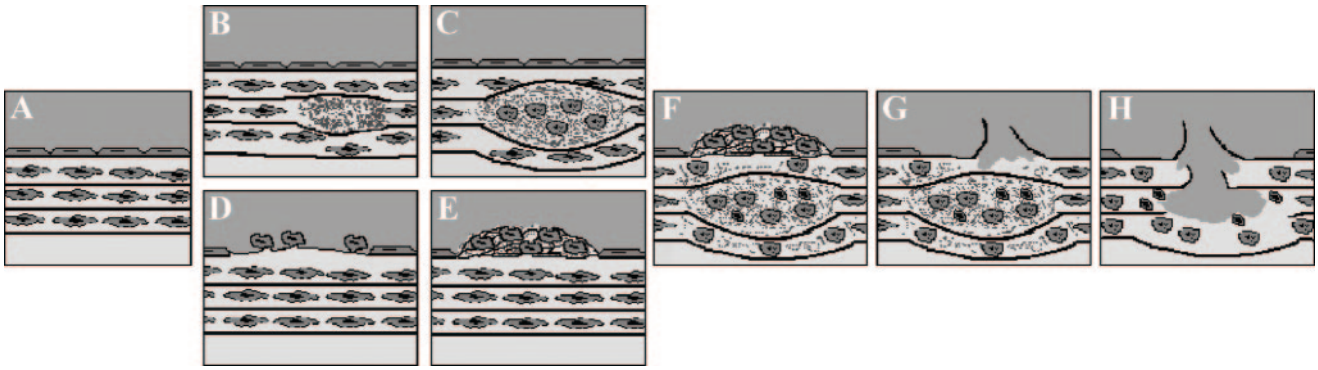

Figure 5. Model for aneurysm formation in *Pkd1* hypomorphic mice. A, Normal vessel wall. The SMCs produce an excessive amount of matrix components, which accumulate between the elastin lamellae (B). SMCs between the disjoined elastin lamellae proliferate increasing the media thickness (C). The endothelial cells detach from the elastin lamellae (D). The number of intima cells increases and the matrix components accumulate in the subendothelial region (E). The combination of a weak aortic media and a tear in the intima leads to (partial) rupture of the vessel wall resulting in intramural bleeding (F–H).

embryos showed increased microvascular permeability at endothelium cell-cell junctions, edema, and hemorrhages.[10,11] All these factors may weaken the intima and alert the shear stress response, making the intima more prone to rupture.

Thus, lowering of *Pkd1* transcription levels induces degenerative alterations in both the intima and media resulting into a dissecting aneurysm. However, intact regions of the aorta were still present in the *Pkd1*$^{nl/nl}$ mice and the overall construction of the aorta with regard to the elastin lamellae is normal. Furthermore, we did not found any abnormalities in these mice at the age of 1 week (data not shown). The elastin assembly may be independent of *Pkd1* expression during development. Matrix components that are involved in elastin organization, like versican, and fibrillin-1, were also not altered compared with the wild-type aortas.[32] This indicates that polycystin1 is probably not implicated in vessel wall development but rather maintains the structural integrity of the vasculature.

Acknowledgments

The authors thank Prof Dr A.C. Gittenberger-de Groot and Dr J.J. Baelde (Leiden University Medical Center) for critical discussions, R. Wolterbeek for statistical support, and W.N. Leonhard and L.J. Wisse for technical assistance.

Sources of Funding

This research was funded by the Netherlands organization for scientific research (NWO/ZonMw 016.036.353) and the Dutch Heart foundation (NHS 2002B177).

Disclosures

None.

References

1. Chapman AB, Rubinstein D, Hughes R, Stears JC, Earnest MP, Johnson AM, Gabow PA, Kaehny WD. Intracranial aneurysms in autosomal dominant polycystic kidney disease. *N Engl J Med*. 1992;327:916–920.
2. Ruggieri PM, Poulos N, Masaryk TJ, Ross JS, Obuchowski NA, Awad IA, Braun WE, Nally J, Lewin JS, Modic MT. Occult intracranial aneurysms in polycystic kidney disease: screening with MR angiography. *Radiology*. 1994;191:33–39.
3. Torra R, Nicolau C, Badenas C, Bru C, Perez L, Estivill X, Darnell A. Abdominal aortic aneurysms and autosomal dominant polycystic kidney disease. *J Am Soc Nephrol*. 1996;7:2483–2486.
4. Chapman JR, Hilson AJ. Polycystic kidneys and abdominal aortic aneurysms. *Lancet*. 1980;1:646–647.
5. Roodvoets AP. Aortic aneurysms in presence of kidney disease. *Lancet*. 1980;1:1413–1414.
6. Muller BT, Modlich O, Prisack HB, Bojar H, Schipke JD, Goecke T, Feindt P, Petzold T, Gams E, Muller W, Hort W, Sandmann W. Gene expression profiles in the acutely dissected human aorta. *Eur J Vasc Endovasc Surg*. 2002;24:356–364.
7. Griffin MD, Torres VE, Grande JP, Kumar R. Vascular expression of polycystin. *J Am Soc Nephrol*. 1997;8:616–626.
8. Peters DJM, van de WA, Spruit L, Saris JJ, Breuning MH, Bruijn JA, De Heer E. Cellular localization and tissue distribution of polycystin-1. *J Pathol*. 1999;188:439–446.
9. Boulter C, Mulroy S, Webb S, Fleming S, Brindle K, Sandford R. Cardiovascular, skeletal, and renal defects in mice with a targeted disruption of the Pkd1 gene. *Proc Natl Acad Sci U S A*. 2001;98:12174–12179.
10. Kim K, Drummond I, Ibraghimov-Beskrovnaya O, Klinger K, Arnaout MA. Polycystin 1 is required for the structural integrity of blood vessels. *Proc Natl Acad Sci U S A*. 2000;97:1731–1736.
11. Muto S, Aiba A, Saito Y, Nakao K, Nakamura K, Tomita K, Kitamura T, Kurabayashi M, Nagai R, Higashihara E, Harris PC, Katsuki M, Horie S. Pioglitazone improves the phenotype and molecular defects of a targeted Pkd1 mutant. *Hum Mol Genet*. 2002;11:1731–1742.
12. Wu G, Markowitz GS, Li L, D'Agati VD, Factor SM, Geng L, Tibara S, Tuchman J, Cai Y, Park JH, van Adelsberg J, Hou H Jr, Kucherlapati R, Edelmann W, Somlo S. Cardiac defects and renal failure in mice with targeted mutations in Pkd2. *Nat Genet*. 2000;24:75–78.
13. Lantinga-van Leeuwen IS, Dauwerse JG, Baelde HJ, Leonhard WN, van der Wal A, Ward CJ, Verbeek S, Deruiter MC, Breuning MH, De Heer E, Peters DJ. Lowering of Pkd1 expression is sufficient to cause polycystic kidney disease. *Hum Mol Genet*. 2004;13:3069–3077.
14. Bergwerff M, Deruiter MC, Hall S, Poelmann RE, Gittenberger-de Groot AC. Unique vascular morphology of the fourth aortic arches: possible implications for pathogenesis of type-B aortic arch interruption and anomalous right subclavian artery. *Cardiovasc Res*. 1999;44:185–196.
15. Melrose J, Whitelock J, Xu Q, Ghosh P. Pathogenesis of abdominal aortic aneurysms: possible role of differential production of proteoglycans by smooth muscle cells. *J Vasc Surg*. 1998;28:676–686.
16. Qian Q, Hunter LW, Li M, Marin-Padilla M, Prakash YS, Somlo S, Harris PC, Torres VE, Sieck GC. Pkd2 haploinsufficiency alters intracellular calcium regulation in vascular smooth muscle cells. *Hum Mol Genet*. 2003;12:1875–1880.
17. Basalyga DM, Simionescu DT, Xiong WF, Baxter T, Starcher BC, Vyavahare NR. Elastin degradation and calcification in an abdominal aorta injury model - Role of matrix metalloproteinases. *Circulation*. 2004;110:3480–3487.
18. Bunton TE, Biery NJ, Myers L, Gayraud B, Ramirez F, Dietz HC. Phenotypic alteration of vascular smooth muscle cells precedes elastolysis in a mouse model of Marfan syndrome. *Circ Res*. 2001;88:37–43.
19. Ibraghimov-Beskrovnaya O, Bukanov NO, Donohue LC, Dackowski WR, Klinger KW, Landes GM. Strong homophilic interactions of the Ig-like domains of polycystin-1, the protein product of an autosomal dominant polycystic kidney disease gene, PKD1. *Hum Mol Genet*. 2000;9:1641–1649.
20. Scheffers MS, van der Bent P, Prins F, Spruit L, Breuning MH, Litvinov SV, De Heer E, Peters DJM. Polycystin-1, the product of the polycystic kidney disease 1 gene, co-localizes with desmosomes in MDCK-cells. *Hum Mol Genet*. 2000;9:2743–2750.
21. Geng L, Burrow CR, Li HP, Wilson PD. Modification of the composition of polycystin-1 multiprotein complexes by calcium and tyrosine phosphorylation. *Biochim Biophys Acta*. 2000;1535:21–35.
22. Davis EC. Smooth-muscle cell to elastic lamina connections in developing mouse aorta - role in aortic medial organization. *Lab Invest*. 1993;68:89–99.
23. Qian Q, Li M, Cai Y, Ward CJ, Somlo S, Harris PC, Torres VE. Analysis of the polycystins in aortic vascular smooth muscle cells. *J Am Soc Nephrol*. 2003;14:2280–2287.
24. Halayko AJ, Solway J. Molecular mechanisms of phenotypic plasticity in smooth muscle cells. *J Appl Physiol*. 2001;90:358–368.
25. Li DY, Brooke B, Davis EC, Mecham RP, Sorensen LK, Boak BB, Eichwald E, Keating MT. Elastin is an essential determinant of arterial morphogenesis. *Nature*. 1998;393:276–280.
26. Molin DG, Poelmann RE, Deruiter MC, Azhar M, Doetschman T, Gittenberger-de Groot AC. Transforming growth factor beta-SMAD2 signaling regulates aortic arch innervation and development. *Circ Res*. 2004;95:1109–1117.
27. Nauli SM, Alenghat FJ, Luo Y, Williams E, Vassilev P, Li X, Elia AE, Lu W, Brown EM, Quinn SJ, Ingber DE, Zhou J. Polycystins 1 and 2 mediate mechanosensation in the primary cilium of kidney cells. *Nat Genet*. 2003;33:129–137.
28. Iomini C, Tejada K, Mo WJ, Vaananen H, Piperno G. Primary cilia of human endothelial cells disassemble under laminar shear stress. *Journal of Cell Biology*. 2004;164:811–817.
29. Van der Heiden K, Groenendijk BC, Hierck BP, Hogers B, Koerten HK, Mommaas AM, Gittenberger-de Groot AC, Poelmann RE. Monocilia on chicken embryonic endocardium in low shear stress areas. *Dev Dyn*. 2006;235:19–28.
30. Ibraghimov-Beskrovnaya O, Dackowski WR, Foggensteiner L, Coleman N, Thiru S, Petry LR, Burn TC, Connors TD, Van Raay TJ, Bradley J, Qian F, Onuchic LF, Watnick TJ, Piontek K, Hakim RM, Landes GM, Germino GG, Sandford R, Klinger KW. Polycystin: In vitro synthesis, in vivo tissue expression, and subcellular localization identifies a large membrane-associated protein. *Proc Natl Acad Sci U S A*. 1997;94:6397–6402.
31. Ilan N, Madri JA. PECAM-1: old friend, new partners. *Curr Opin Cell Biol*. 2003;15:515–524.
32. Isogai Z, Aspberg A, Keene DR, Ono RN, Reinhardt DP, Sakai LY. Versican interacts with fibrillin-1 and links extracellular microfibrils to other connective tissue networks. *J Biol Chem*. 2002;277:4565–4572.